

EVALUATION OF THE IMPACT OF STRUCTURAL MODEL VARIABILITY ON TRANSONIC AEROELASTICITY

S. Marques¹, K.J. Badcock¹, H. Khodaparast¹, and J.E.Mottershead¹

¹Department of Engineering
University of Liverpool
L69 3BX, U.K.
K.J.Badcock@liverpool.ac.uk

Keywords. Transonic Aeroelasticity, Structural Variability, CFD.

Abstract. Transonic aeroelasticity requires CFD level aerodynamics for first principals prediction. This also brings a computational cost, which is overcome in the current paper by the use of eigenvalue based solution methods which avoid the need for time domain simulation. Simulation tools need to be able to predict the influence of variability from model components to be widely useful. In this paper the variability considered arises from the structural model. A systematic study is carried out for the significance of the routes of impact from structural variability, namely through the normal mode frequencies and mode shapes, and from the aerostatic solution. The Goland wing and a jet transport wing are used as test cases, and it is shown that most of the useful information can be obtained efficiently from the normal mode frequency variation if the analysis is done about the mean structural aerostatic solution.

1 INTRODUCTION

Considerable effort has been put into the problem of simulating transonic aeroelastic response based on CFD level aerodynamics. The approaches were initially in the time domain, but a research effort has been directed to developing reduced order models which retain the important physics (and in particular can represent nonlinearity). More recently these reduced order models have been used to assess the impact of structural variability. The approach typically used is to build a reduced order model of the aerodynamics, and then to couple this to structural models that have been generated from randomised parameters.

There are three ways in which structural variability can influence the aeroelastic response. First, the distribution of normal mode frequencies changes the stability characteristics. This influence will be contained in a Monte Carlo simulation based on a reduced aerodynamic model built at mean parameter structural mode shapes if the range of frequencies is used in the training. Secondly, the mode shapes will also vary. This effect is typically not in the reduced order aerodynamic model built using the mean parameter structural model, with the assumption being that the aerodynamic response can still be represented well when the structural modes change. Thirdly, the aerostatic solution also changes with the structural parameters, and this could impact significantly on the reduced order model built for the steady state at the mean parameters.

This paper will investigate the relative importance of these effects. The investigation is based on an eigenvalue analysis which allows rapid evaluation of linear stability. This approach has already been used to compute a Monte-Carlo simulation of the Goland wing

with 1000 samples being computed overnight on a PC, including CFD level aerodynamics. This level of performance allows the study of the influence of the three ways that the variability can impact the aeroelastic response. The Goland and MDO wings are used as test cases.

2 AEROELASTIC STABILITY FORMULATION

The semi-discrete form of the coupled CFD-FEM system is written as

$$\frac{d\mathbf{w}}{dt} = \mathbf{R}(\mathbf{w}, \mu) \quad (1)$$

where

$$\mathbf{w} = [\mathbf{w}_f, \mathbf{w}_s]^T \quad (2)$$

is a vector containing the fluid unknowns (\mathbf{w}_f) and the structural unknowns (\mathbf{w}_s), and

$$\mathbf{R} = [\mathbf{R}_f, \mathbf{R}_s]^T \quad (3)$$

is a vector containing the fluid residual (\mathbf{R}_f) and the structural residual (\mathbf{R}_s). In the current work the structure is modelled by a small number of modes. The residual also depends on a parameter μ (in this paper μ is altitude) which is independent of \mathbf{w} . An equilibrium $\mathbf{w}_0(\mu)$ of this system satisfies $\mathbf{R}(\mathbf{w}_0, \mu) = \mathbf{0}$.

The linear stability of equilibria of equation 1 is determined by eigenvalues of the Jacobian matrix $A = \partial\mathbf{R}/\partial\mathbf{w}$. The details of the Jacobian calculation are given in references [1, 2]. Write the coupled system eigenvalue problem as

$$\begin{bmatrix} A_{ff} & A_{fs} \\ A_{sf} & A_{ss} \end{bmatrix} \mathbf{p} = \lambda \mathbf{p} \quad (4)$$

where \mathbf{p} and λ are the complex eigenvector and eigenvalue respectively. Partition the eigenvector as

$$\mathbf{p} = [\mathbf{p}_f, \mathbf{p}_s]^T \quad (5)$$

The eigenvalue λ satisfies [3] the nonlinear eigenvalue problem

$$S(\lambda)\mathbf{p}_s = \lambda\mathbf{p}_s \quad (6)$$

where $S(\lambda) = A_{ss} - A_{sf}(A_{ff} - \lambda I)^{-1}A_{fs}$. The solution of this problem is discussed in reference [4], and is based on an approximation to the matrix $(A_{ff} - \lambda I)^{-1}$ given by

$$(A_{ff} - \lambda I)^{-1} = A_{ff}^{-1} + \lambda A_{ff}^{-1} A_{ff}^{-1} + \dots \quad (7)$$

This series converges for small values of λ , and so in practice a shift is used to ensure this condition. The details of how to define the shift are described in reference [4] and will not be considered further here.

There are a number of dependencies and options for this nonlinear eigenvalue problem that we want to bring out. To do this define the residual of the problem as

$$\mathbf{E}(\mathbf{w}_0, \lambda, \mathbf{p}_s, \phi, \omega) = (A_{ss} - A_{sf}(A_{ff} - \lambda I)^{-1}A_{fs})\mathbf{p}_s - \lambda\mathbf{p}_s \quad (8)$$

Note the dependence of this residual on the static solution \mathbf{w}_0 through all of the Jacobian matrices. Also the residual depends on the structural normal mode shapes ϕ through the matrices A_{ss} , A_{sf} and A_{fs} , and the structural normal mode frequencies ω through the matrix A_{ss} . Also, this residual can be computed through one linear solve with the matrix $(A_{ff} - \lambda I)$ against the right hand side $A_{fs}\mathbf{p}_s$, which represents a manageable cost. Write the the series approximation to this residual as

$$\mathbf{E}_s(\mathbf{w}_0, \lambda, \mathbf{p}_s, \phi, \omega) = (A_{ss} - A_{sf}(A_{ff}^{-1} + \lambda A_{ff}^{-1}A_{ff}^{-1})A_{fs})\mathbf{p}_s - \lambda\mathbf{p}_s, \quad (9)$$

which, after the pre-computation of the series coefficients A_{ff} , can be evaluated very cheaply. The solution vector for the nonlinear eigenvalue problem is written as $\mathbf{w}_e = [\mathbf{p}_s, \lambda]^T$. Then, two options are available to solve the nonlinear eigenvalue problem. Both employ Newton's method driven by the Jacobian matrix $\partial\mathbf{E}_s/\partial\mathbf{w}_e$ which can be evaluated rapidly. The first uses the residual \mathbf{E} and the second option uses the approximate residual \mathbf{E}_s . It was shown in reference [4] that the approximate residual can give good results at the cost of the initial precomputation of the series.

In reference [5] the influence of structural variability was considered. It was assumed that a small number of structural parameters are uncertain, in either a probabilistic or interval sense. This leads to the requirement to solve the nonlinear eigenvalue problem at a number of different normal mode and frequency sets. This is done by solving against the residual $\mathbf{E}(\mathbf{w}_0, \lambda, \mathbf{p}_s, \phi_j, \omega_j)$ at the normal mode shapes and frequencies evaluated at the j th realisation of the uncertain structural parameters, using the series Jacobian approximation $\partial\mathbf{E}_s(\mathbf{w}_0, \lambda, \mathbf{p}_s, \bar{\phi}, \bar{\omega})/\partial\mathbf{w}_e$ where the notation $\bar{\phi}, \bar{\omega}$ indicates the mode set evaluated at the mean uncertain structural parameters. In other words, the series approximation to the Jacobians is evaluated at the mean structural parameters and is then used to drive the Newton solution for every realisation of the uncertain structural normal modes.

We want to calculate the solutions to the nonlinear eigenvalue problem for matched calculations to locate where in the envelope eigenvalues with a positive real part (i.e. instability) might be encountered. The most convenient way of doing this is to fix the Mach number and incidence, and to vary the altitude to change the velocity and density in a matched way. Then, in previous work, the series approximation is computed at a high altitude (with the normal mode frequencies as shifts), and the nonlinear eigenvalue problem convergence is then driven by these matrices as the altitude is decreased towards the ground. In this way the modification of each normal mode eigenvalue in the aeroelastic system can be traced as a function of altitude. In addition, any modes which show a tendency to instability can be examined for the influence of structural variability, again exploiting the series approximation already computed.

There are two additional questions that we consider in the current paper. First, in general the steady state \mathbf{w}_0 depends on the altitude also. This was neglected in previous work and the wing was held at its rigid shape for the calculation of the steady state. The inclusion of the static deflection requires at least the updating of the residual \mathbf{E} at the correct static equilibrium, and possibly also the updating of the series approximation if the change in the equilibrium is too large.

The second additional question relates to the calculation of the influence of uncertainty. The inclusion of aerostatic equilibrium effects introduces an additional route for the structural uncertainty to influence the aeroelastic eigenvalues. These routes can be summarised as

1. Normal mode frequency - the variability changes the normal mode frequencies
2. Normal mode shape - the variability changes the normal mode shapes
3. Static equilibrium - the change of normal mode shapes and frequencies changes the static equilibrium.

In the current notation the following scenarios can be considered by applying the approach described above for treating structural variability in the following ways:

- Route 1 can be computed by solving the nonlinear eigenvalue problem defined by the residual $\mathbf{E}_s(\bar{\mathbf{w}}_0, \lambda, \mathbf{p}_s, \bar{\phi}, \omega_j)$. The series residual is evaluated at the j th realisation of the normal mode frequency, but at the mean structural parameter normal modes and the equilibrium \mathbf{w}_0 calculated at the mean normal modes and frequencies.
- Routes 1 and 2 combined can be computed by solving the nonlinear eigenvalue problem defined by the residual $\mathbf{E}(\bar{\mathbf{w}}_0, \lambda, \mathbf{p}_s, \phi_j, \omega_j)$. This was the problem solved in reference [5], and used the mean parameter equilibrium \mathbf{w}_0 , and the j th realisation of both the normal mode frequencies and mode shapes.
- Routes 1-3 can be combined by solving the nonlinear eigenvalue problem defined by the residual $\mathbf{E}(\mathbf{w}_{0j}, \lambda, \mathbf{p}_s, \phi_j, \omega_j)$. In this case the equilibrium is also evaluated at the j th realisation of the normal mode shapes and frequencies.

If route 1 dominates, then a very efficient method is obtained for calculating the influence of structural model variability. The method for route 1 would be far more efficient than the method demonstrated in reference [5] for routes 1 and 2. Hence, the first objective of this paper is to consider the importance of route 2. Finally, the importance of route 3 is also considered.

3 RESULTS

3.1 Clean Goland Wing

The Goland wing is a model wing which has a chord of 6 feet and a span of 20 feet. It is a rectangular cantilevered wing with a 4% thick parabolic section. The structural model follows the description given in reference [6]. Four mode shapes were retained for the aeroelastic simulation. The eigenvalue formulation given in the previous section was evaluated for the Goland wing test case in reference [4]. The CFD grid is block structured and uses an O-O topology. This allows points to be focussed in the tip region which is most critical for the aerodynamic contribution to the aeroelastic response. The fine grid has 236 thousand points and a coarse level was extracted from this grid, which has 35 thousand points. The wing structure is composed of upper and lower skins, three spars with caps, eleven ribs with caps and 33 posts. There are two versions of the wing which are considered, namely with and without a tip store. The wing without a tip store is referred to as clean. The tip store is added to the clean wing by including a point mass at some streamwise location at the wing tip. The baseline tip mass configuration has the mass located 0.25 ft from the leading edge. In both cases the parameters which define the geometry of the structural model are the thicknesses of the skins, the areas of the spar and rib caps, the thicknesses of the spars and ribs and the areas of the posts. The mean values of these parameters follow those given in reference [7]. It should be noted that the density of the structural elements was taken to be negligible and the inertial properties are modelled as lumped mass elements. As a consequence the mass and stiffness properties of the wing are decoupled.

The sensitivity of the linear flutter speed to the parameters in the structural model was calculated and the seven most important structural parameters selected. These are the thicknesses of the leading and trailing edge spars, the upper and lower skin thicknesses and the areas of the leading edge, trailing edge and centre spar caps. These parameters were varied randomly with a coefficient of variation of 0.05. The results were reported in reference [5], where the angle of attack used was zero, and combined with the symmetry of the Goland wing, this meant that the static equilibrium was always the same as the rigid wing shape.

For the current results we start by considering a Mach number of 0.5 and a small non-zero incidence (0.8 degrees) to introduce a static deflection which depends on altitude. The solution at 9000ft is shown in figure 1 and features almost a pure bending deflection of approximately one thickness at the wing tip. The mode tracking for the normal modes in the aeroelastic system is shown in figure 2. The first wing bending and torsion modes interact. The eigenvalues are shown in the figure with the aerostatic deformation effect included. The eigenvalues when keeping the static wing solution rigid shows flutter about 500ft lower than when the aerostatic deformation effect is included. Note that from the plot of the imaginary part of the eigenvalues, the two modes that are interacting have frequencies that have virtually merged by the flutter altitude.

These results were obtained for the mean structural parameters. Next a Monte Carlo simulation was carried out. One thousand samples were generated based on the randomisation of the crucial seven structural parameters. Here a sample consists of the four normal shape shapes and frequencies. The mean behaviour indicated that the first wing torsion mode was the one to become unstable. The series approximation was generated about the mean flutter altitude with a shift given by the frequency at the crossing. This series was then used to drive convergence for the nonlinear eigenvalue solves. The spread of samples for the real part of the eigenvalue at the mean flutter altitude is shown in figure 3(b). Included in this figure are the mean real part traces showing the cases with the static deformation crossing the imaginary axis at a higher altitude. The spread of the samples for the cases with and without the aerostatic deformation show a similar spread of points, with the distribution shifted by a similar amount to the mean parameter values. This is shown by the PDF in figure 3. Note that in this figure the PDF's below the mean value have been corrupted due to the nonlinear eigenvalue solver converging to the wrong eigenvalue. The eigenvectors in this case for the first two modes are very close, making the convergence rather sensitive. However, the important information in the plots is the distribution above the mean value (i.e. more unstable) and this is not influenced by this convergence behaviour. Finally, the Monte Carlo simulation for the deformed aerostatic solution was rerun based on the series solution for the nonlinear eigenvalue residual.

To express these results in the terms of the previous section, routes 1-3 and route 1 give similar results for the PDF, indicating that the changes to normal mode frequencies dominates the aeroelastic eigenvalue real part variability as opposed to aerostatic deformation and normal mode variability. This could be explained by the closeness of the aeroelastic eigenvalue imaginary parts, which might make the damping very sensitive to changes in the normal mode frequencies in this case.

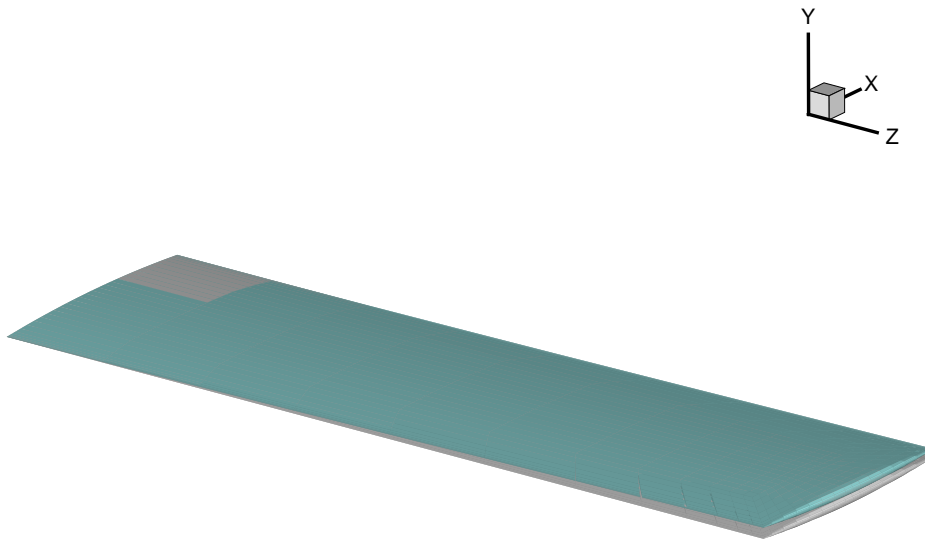
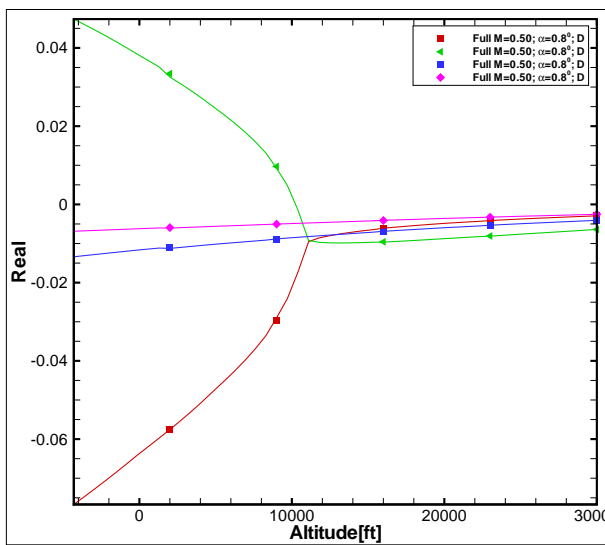
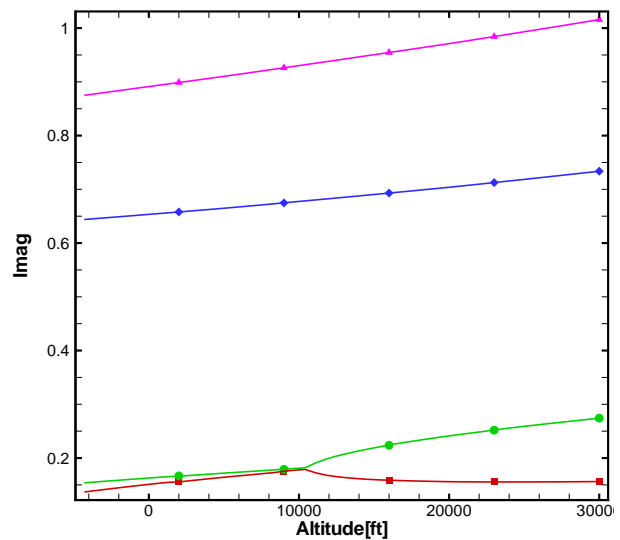


Figure 1: Views of the aerostatic solution for the clean Golang Wing at the mean structural parameters and $\alpha = 0.8^\circ$, $M=0.5$.



Eigenvalue (Deformed) - Real part



Eigenvalue (Deformed) - Imaginary part

Figure 2: Mode tracking for the clean Golang Wing at the mean structural parameters and $\alpha = 0.8^\circ$, $M=0.5$. Here Deformed refers to the wing shape used to generate the matrices i.e. the aerostatic equilibrium at each altitude.

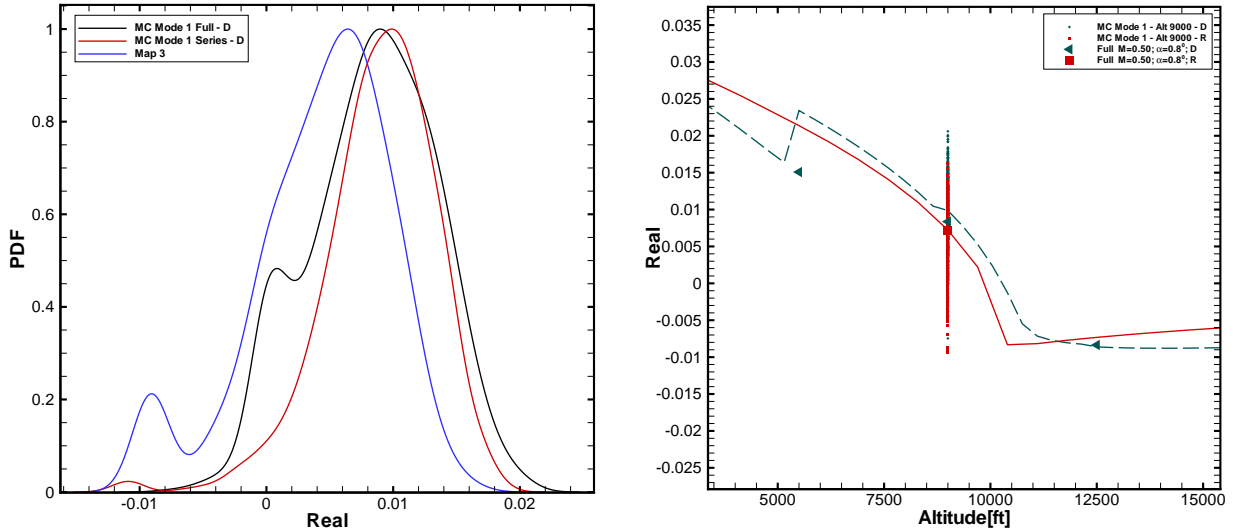


Figure 3: PDF and real part spread for the clean Goland Wing with and without static deformation at 9000 ft and $\alpha = 0.8^\circ$, $M=0.5$.

3.2 Goland Wing with Wing Tip Store

Next we consider a transonic case at Mach 0.9 and 1 degree of incidence for the Goland wing with tip store. These calculations were started at 40 thousand feet since for the mean structural parameter case the wing is unstable below 30000 feet for the wing with the rigid steady state. The aerostatic solution tends to make the shock wave weaker, as shown in figure 4, and this has a stabilising effect for the flutter, shifting the flutter altitude to around 23000 ft. The comparison of the mode tracking for the rigid and aerostatic steady states is shown in figure 5 and beneficial effect of the static deflection on the mean parameter eigenvalues is clear. The real part eigenvalue PDF for the unstable mode is shown in figure 6 together with the spread of samples. There are two comments on this figure. First, the influence of the static deflection can be seen as a translation in the PDF. This indicates that the difference in the flow solutions is not large from the deflection. Secondly, the route 1 PDF (taking account of the normal mode frequency variation and not the mode shape variation) is narrower than the route 1-3 PDF. This is in contrast to the case shown above for the clean wing where the two were in almost perfect agreement. This indicates that in the present case the influence of the mode shape variation is also important, and this could be because the mean parameter aeroelastic imaginary parts are not so close together as before. Also, note that the variation is smaller in this case.

3.3 MDO Wing

The final case we consider is the MDO wing which is representative of a commercial transport wing with a span of 36m. The wing has a thick supercritical section. The structure is modelled by a wing box. Eight modes were retained for the current analysis in the range 0.6 to 4 Hz. Previous results have been shown in reference [4]. The section is not symmetric and static deflections have been seen to be significant. Calculations were run at Mach 0.8 and 3 degrees of incidence. The static deflection resulting at sea level is shown in figure 7. Pressure contours are shown in figure 8 and show that again the static solutions are similar. There are small modifications to the location and strength of the shock wave. The wing structure is supported by spring elements at the root and these elements are the most important for determining flutter. The values of the spring

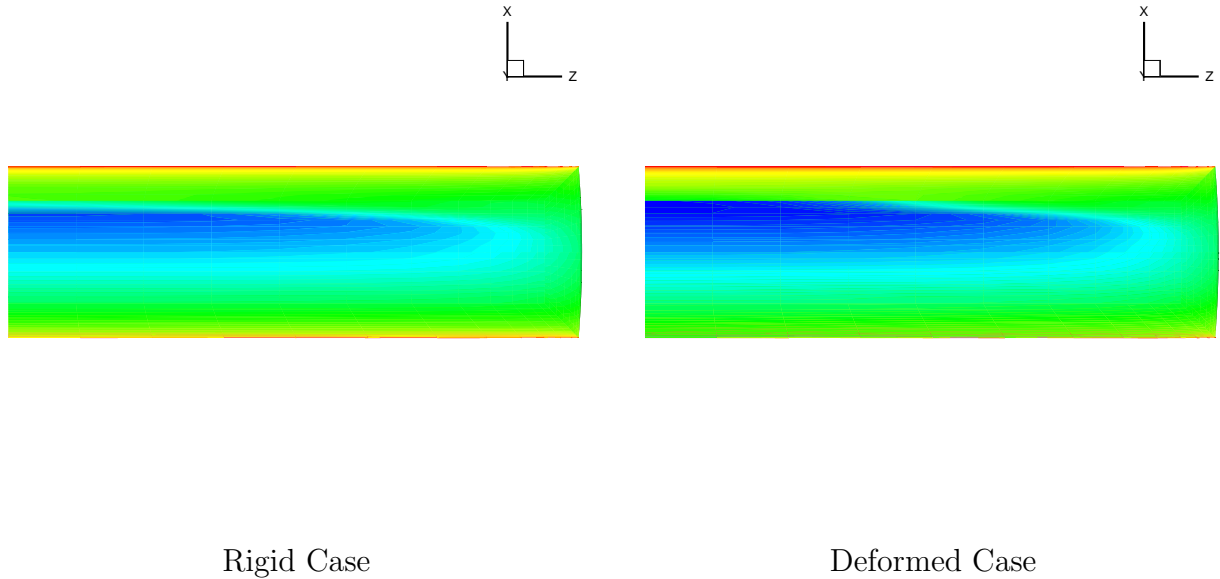


Figure 4: Pressure contours for the Goland Wing with tip store, $\alpha = 1^\circ$, $M=0.9$.

constants are varied by three orders of magnitude for the Monte Carlo simulation [8].

The mean structural parameter aeroelastic eigenvalue tracking is shown in figure 9. No flutter is experienced in the altitude range which extends to 5000m below sea level, as might seem reasonable for a case which is meant to be representative of a transport wing. Modes 6 and 7 are interacting at the lowest altitude although they remain damped. The aeroelastic eigenvalue imaginary parts for the interacting modes are much further apart than for both of the Goland cases. Based on the aerostatic equilibrium, the spread and PDF of 100 samples including routes 1 and 1-3 is shown in figure 10. There is a slight discrepancy in the location of the mean, probably due to the systematic error introduced by the series solution. Apart from this the width of the distribution is almost identical between routes 1 and 1-3. This could indicate that the flow solution is not sensitive to small changes in the important modes.

4 CONCLUSIONS

This paper has considered the routes through which structural variability can impact on aeroelastic stability. An aeroelastic eigenvalue solver that can separate out the different routes was used. In the first set of results, for the clean Goland wing at subsonic conditions, the key route seemed to be through the variation in normal mode frequencies. Comparison of the real part aeroelastic eigenvalue PDF's showed little additional influence from the mode shape variation and the aerostatic equilibrium. This behaviour was explained by how close the aeroelastic eigenvalue imaginary parts are at flutter. In contrast, a transonic case with a tip store showed some influence of the mode shape variation, possibly because the imaginary parts at flutter were further apart on this case, and also because the shock is sensitive to the mode shape variations. Finally, the spread of results for the MDO wing, prior to flutter in this case, showed that the variation due to the variation in frequencies could account for the flutter variability, possibly in this case because small changes in the mode shapes do not significantly impact on the aerodynamics.

The conclusion from these results is that route 1 accounts for most of the variability

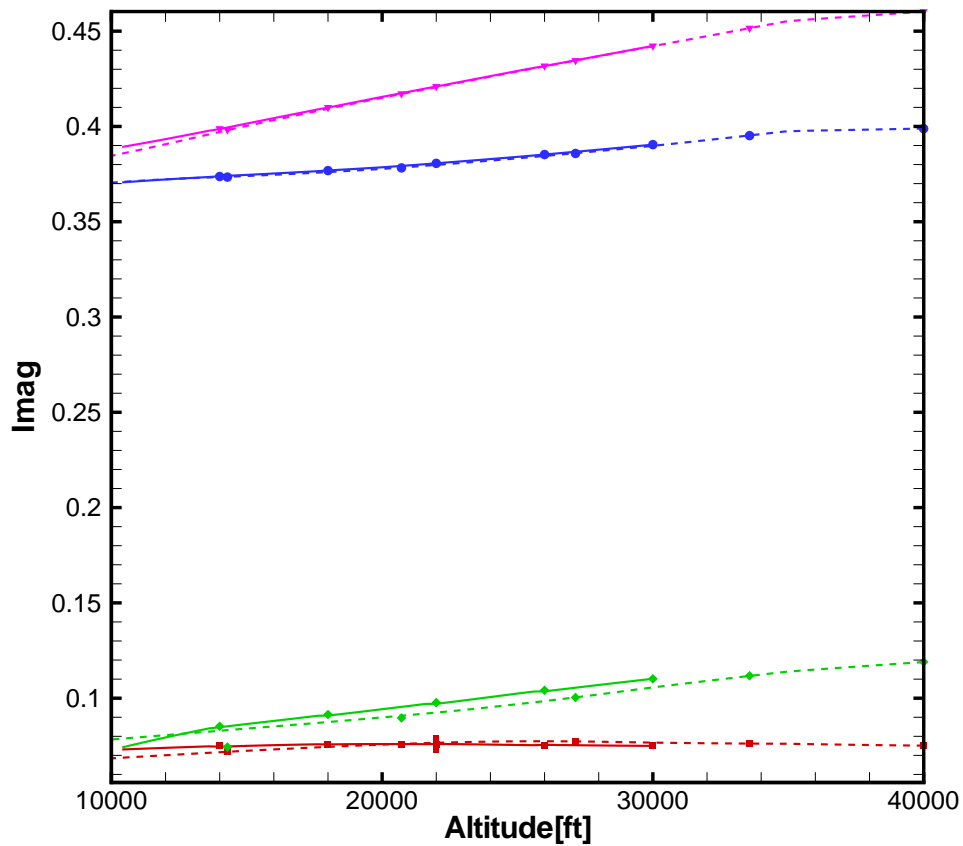
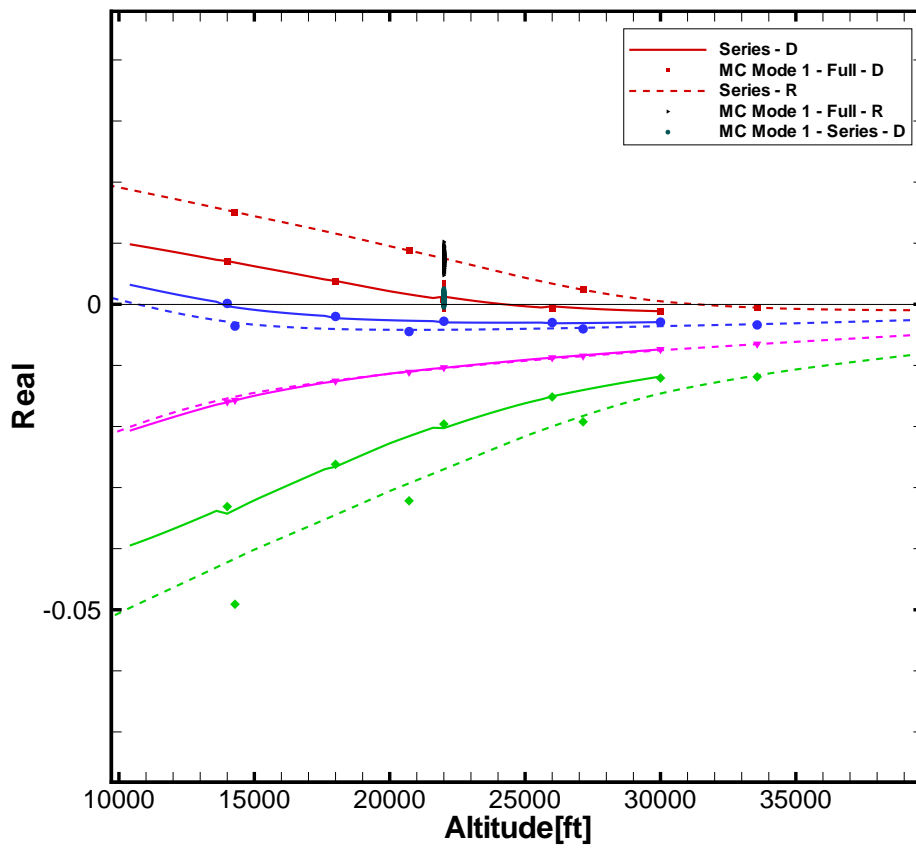


Figure 5: Mode tracking for the aerostatic solution for the Goland Wing with tip store at the mean structural parameters and $\alpha = 1^\circ$, $M=0.9$.

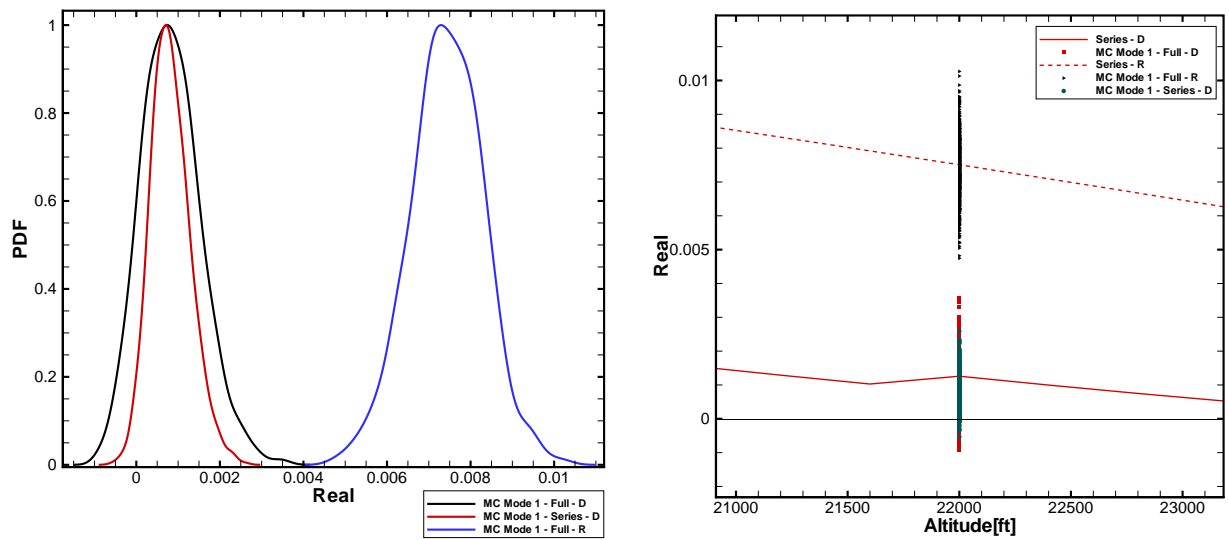


Figure 6: PDF and spread of the eigenvalue real part at 22000 ft for the Goland Wing with tip store, $\alpha = 1^\circ$, $M=0.9$.

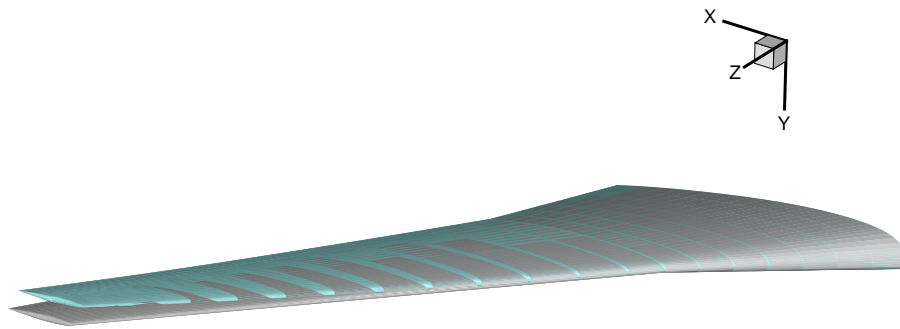


Figure 7: Views of the aerostatic solution for the MDO Wing at the mean structural parameters and $\alpha = 3^\circ$, $M=0.8$.

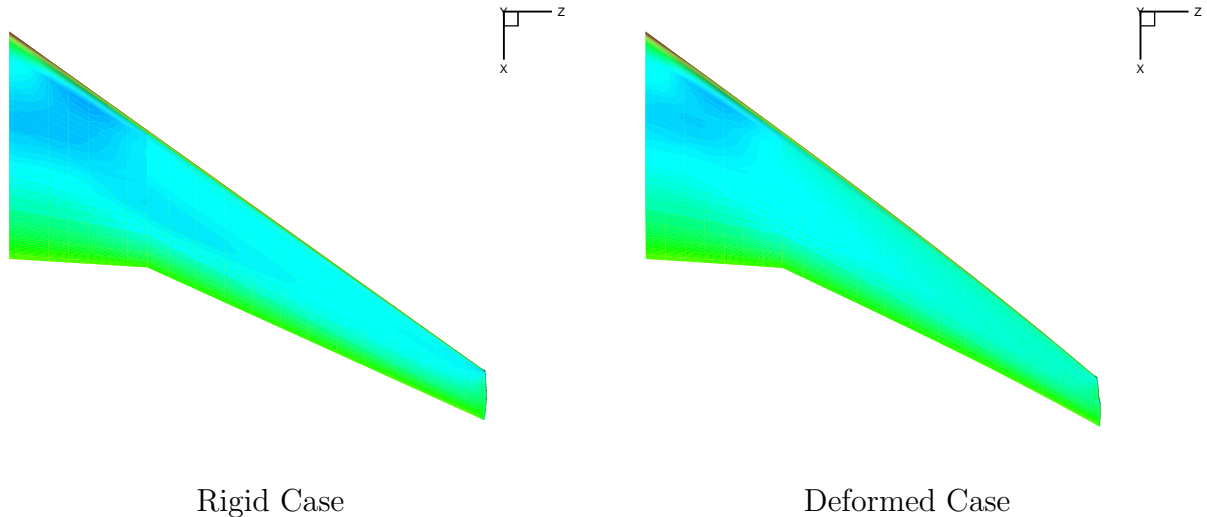


Figure 8: Views of the pressure contours for the MDO Wing at the mean structural parameters and $\alpha = 3^\circ$, $M=0.8$.

in the flutter behaviour. This is a practically useful conclusion since route 1 can be analysed using the series approximation which significantly reduces the computational cost. The variation of mode shapes can however modify the PDF of the aeroelastic real part eigenvalue when the aerodynamics is sensitive to this variation, perhaps when shock waves are important. This may not be very important however since there is likely to be significant uncertainty in the structural variability itself.

Future work will focus on how to account for the dependence of the series approximation to the Schur matrix on its variables. This will allow a systematic investigation for instability across the flight envelope.

5 ACKNOWLEDGEMENTS

This work is funded by the European Union for the Marie Curie Excellence Team ECERTA under contract MEXT-CT-2006 042383.

6 REFERENCES

- [1] Badcock, K.J., M.A. Woodgate, M.A. and Richards, B.E., The Application of Sparse Matrix Techniques for the CFD based Aeroelastic Bifurcation Analysis of a Symmetric Aerofoil, *AIAA Journal*, 42(5), 883-892, May, 2004.
- [2] Badcock, K.J., Woodgate, M.A. and Richards, B.E., Direct Aeroelastic Bifurcation Analysis of a Symmetric Wing Based on the Euler Equations, *Journal of Aircraft*, 42(3),731-737, 2005.
- [3] Bekas, K. and Saad, Y., Computation of Smallest Eigenvalues using Spectral Schur Complements, *SIAM Journal of Scientific Computing*, 27(2), 2005, 458-481.
- [4] Badcock, K.J. and Woodgate, M.A., Prediction of Bifurcation Onset of Large Order Aeroelastic Models, 49th Structural Dynamics and Materials Conference, Schaumburg, Illinois, May, 2008, AIAA-2008-1820.

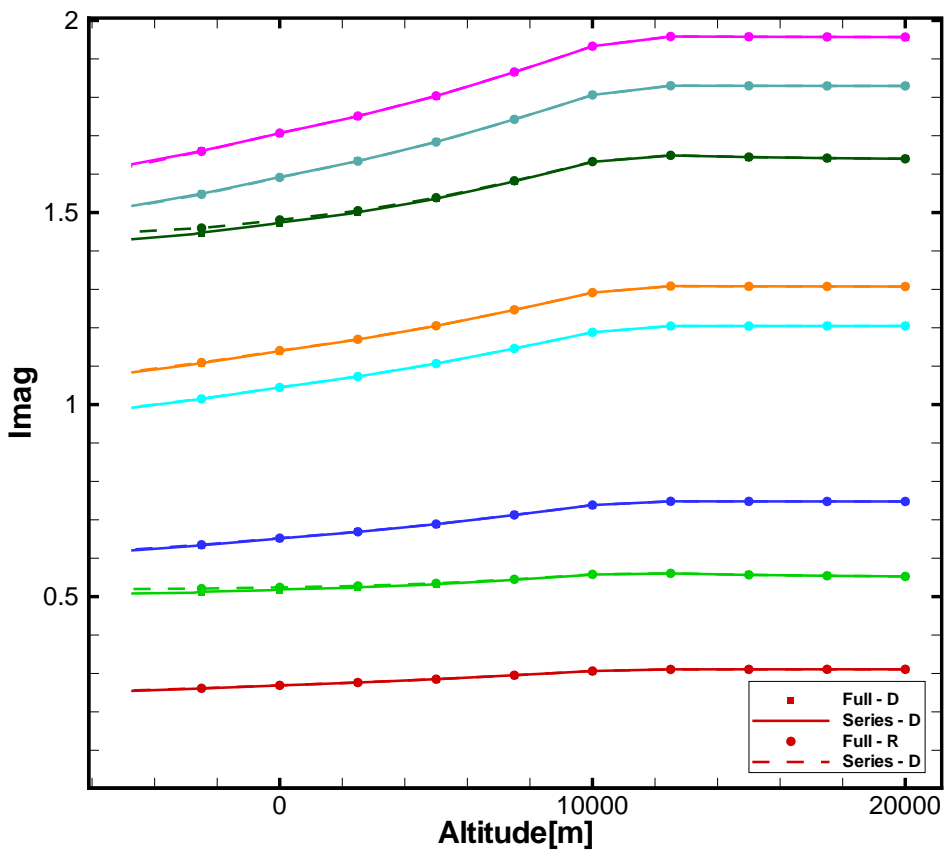
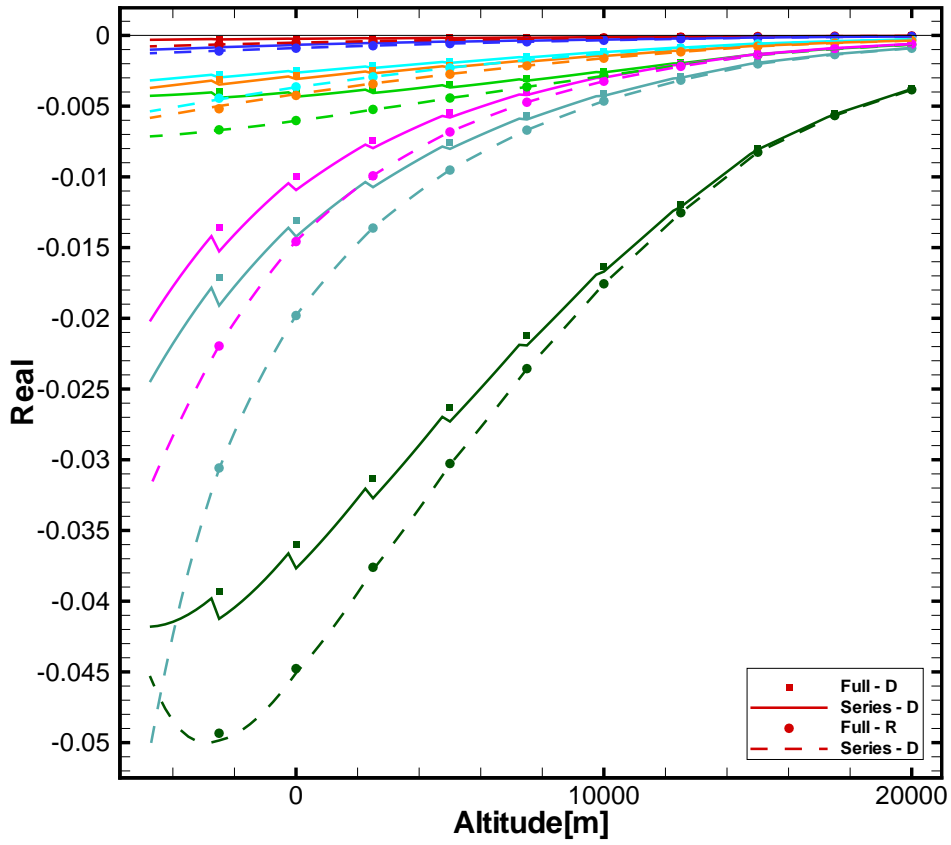


Figure 9: Views of the mode tracking for the MDO wing at $\alpha = 3^\circ$, $M=0.8$.

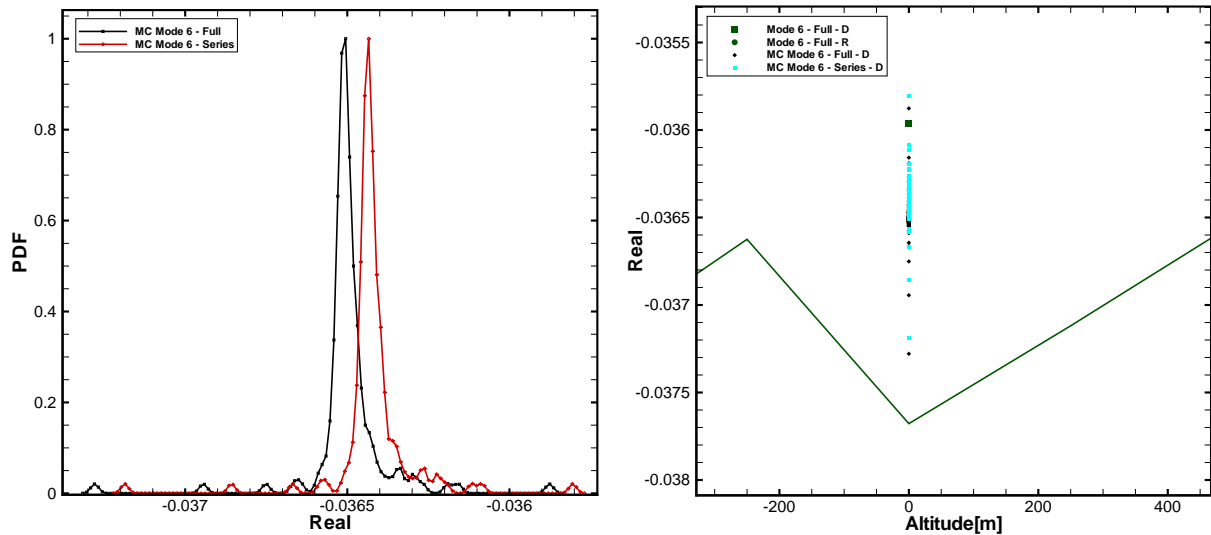


Figure 10: Real Part spread of the 6th aeroelastic mode for the MDO wing at sea level, $\alpha = 3^\circ$, $M=0.8$.

- [5] Marques, S., Badcock, K.J., Khodaparast, H.H. and Mottershead, J.E., CFD Based Aeroelastic Stability Predictions Under the Influence of Structural Variability, 50th Structural Dynamics and Materials Conference, Palm Springs, May, 2009, AIAA-2009-2324.
- [6] Beran, P.S., Knot, N.S., Eastep, F.E., Synder, R.D. and Zweber, J.V., Numerical Analysis of Store-Induced Limit Cycle Oscillation, Journal of Aircraft, 41(6), 1315-1326, 2004.
- [7] Kurdi M, Lindsley N and Beran P, Uncertainty quantification of the Goland wing's flutter boundary, AIAA Paper 2007-6309, August 20-22.
- [8] Haddad Khodaparast, H., Marques, S., Badcock, K.J., Mottershead, J.E, Estimation of Flutter Boundaries in the Presence of Structural Uncertainty by Probabilistic and Fuzzy Methods, International Conference on Structural Engineering Dynamics, 2009, Ericeira, Portugal, 22-24 June, 2009.